Antikaon absorption in the nuclear medium: the role of hadron self-energies and implications for kaonic atoms

Jaroslava Óbertová

Faculty of Nuclear Sciences and Physical Engineering, Czech Technical University in Prague

in collaboration with

Àngels Ramos	**Eliahu Friedman**	**Jiří Mareš**
University of Barcelona	*Hebrew University, Jerusalem*	*NPI, Řež*

15th International Conference on Hypernuclear and Strange Particle Physics, HYP2025,

29 September - 3 October 2025, Tokyo, Japan

K^-N interactions

K^-p scattering:

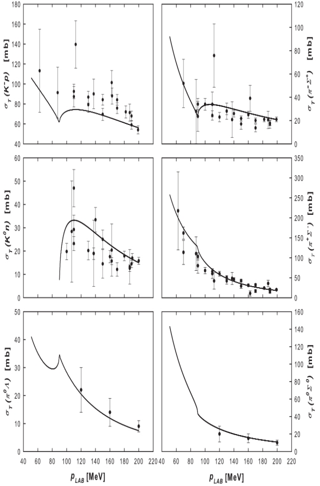

Threshold branching ratios:

$$\gamma = \frac{\Gamma(K^-p \to \pi^+\Sigma^-)}{\Gamma(K^-p \to \pi^-\Sigma^+)} = 2.36 \pm 0.04$$

$$R_c = \frac{\Gamma(K^-p \to \mathrm{charged})}{\Gamma(K^-p \to \mathrm{all})} = 0.664 \pm 0.011$$

$$R_n = \frac{\Gamma(K^-p \to \pi^0\Lambda)}{\Gamma(K^-p \to \mathrm{neutral})} = 0.189 \pm 0.015$$

Kaonic hydrogen:

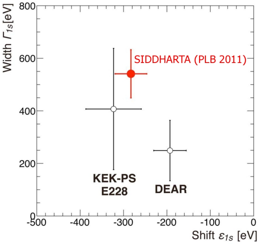

- K^-p data well described by several chiral models

  A. Cieplý, M. Mai, U.-G. Meissner, J. Smejkal, NPA 945 (2016) 17

Free-space $K^- p$ amplitudes in various chiral models

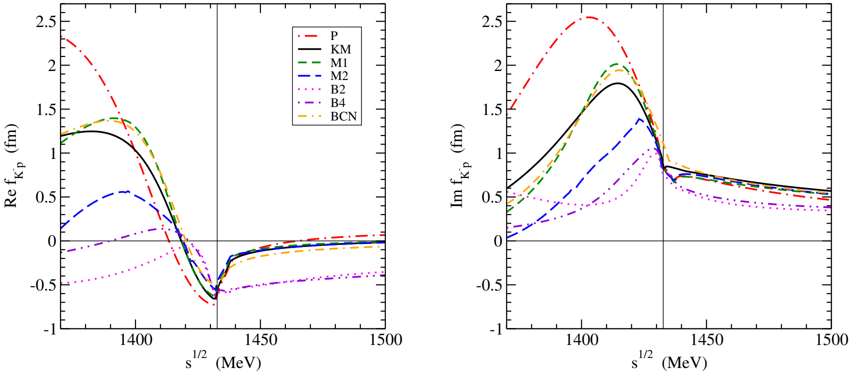

Prague (P)	*A. Cieply, J. Smejkal, Nucl. Phys. A 881 (2012) 115*
Kyoto-Munich (KM)	*Y. Ikeda, T. Hyodo, W. Weise, Nucl. Phys. A 881 (2012) 98*
Murcia (M1 and M2)	*Z. H. Guo, J. A. Oller, Phys. Rev. C 87 (2013) 035202*
Bonn (B2 and B4)	*M. Mai, U.-G. Meißner, Nucl. Phys. A 900 (2013) 51*
Barcelona (BCN)	*A. Feijoo, V. Magas, A. Ramos, Phys. Rev. C 99 (2019) 035211*

Free-space $K^- n$ amplitudes

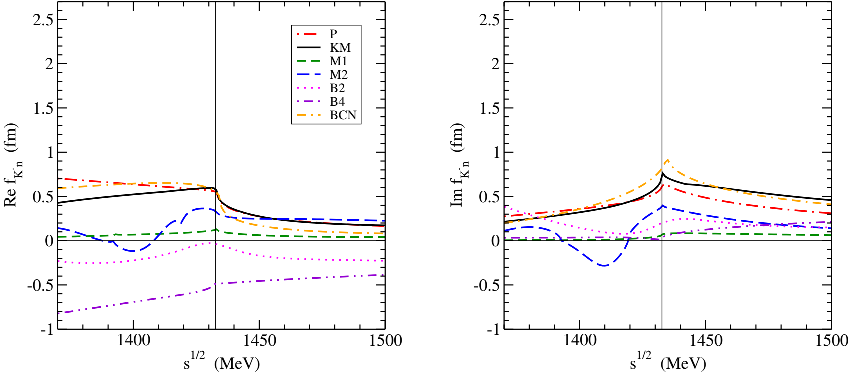

- Measurement of kaonic deuterium by SIDDHARTA-2 Collabortion could provide new constrain on $K^- N$ interaction in $I = 1$ channel

  F. Sgaramella et al. [SIDDHARTA-2], NC C 47 (2024) 285

Kaonic atoms

- Info about $K^- N$ interaction below threshold provided by kaonic atoms

  65 data points (energy shifts, widths, yields=upper level widths) from CERN, Argonne, RAL, BNL
- Global analysis of kaonic atom data using phenomenological potential $\rightarrow \mathrm{Re}\, V_{K^-}(\rho_0) \sim -(150-200)$ MeV

  E. Friedman, A. Gal, PR 452 (2007) 89
- K^- potential from chiral models $\rightarrow \mathrm{Re}\, V_{K^-}(\rho_0) \sim -(40-60)$ MeV

  A. Cieplý, E. Friedman, A. Gal, J. Mareš, NPA 696 (2001) 173

- Chirally motivated models fail to describe kaonic atom data

  E. Friedman, A. Gal, NPA 959 (2017) 66

model	B2	B4	M1	M2	P	KM
$\chi^2(65)$	1174	2358	2544	3548	2300	1806

Multinucleon processes

- Chiral models include only $K^- N \to \pi Y$ ($Y = \Lambda, \Sigma$) decay channel
- K^- interactions with two and more nucleons should be included, (e.g., $K^- + N + N \to Y + N$) $\leftarrow$ analysis of kaonic atom data
  E. Friedman, A. Gal, NPA 959 (2017) 66

$$V^{\mathrm{phen}}_{K^-\mathrm{multiN}} = -4\pi B(\frac{\rho}{\rho_0})^{\alpha}\rho$$

B is a complex amplitude, ρ is nuclear density distribution, ρ_0 is saturation density and α is positive

- equally good description of data with $\chi^2/\mathrm{dof} \leq 2$

Single- vs. multi-nucleon processes

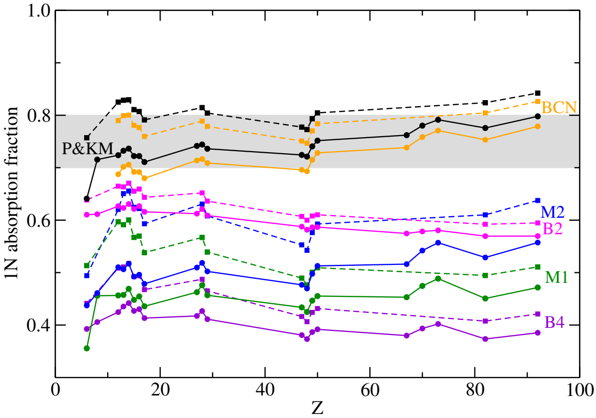

- Fraction of *single-nucleon* absorption 0.75 ± 0.05 (average value, gray band) used as an additional constraint.

→ Only P, KM and BCN models found acceptable in kaonic atom analysis

E. Friedman, A. Gal, NPA 959 (2017) 66

AMADEUS@DAΦNE

K. Piscicchia et al., PLB 782 (2018) 339

$$|f^{s}_{ar}| = (0.334 \pm 0.018\,\mathrm{stat}\,^{+0.034}_{-0.058}\mathrm{syst})\,\mathrm{fm}\,.$$

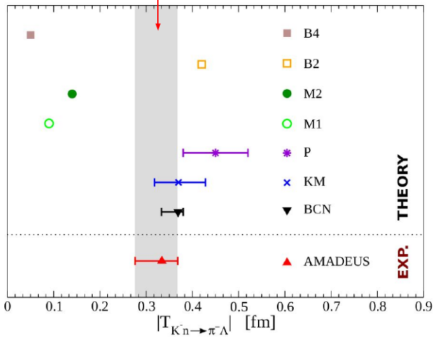

K. Piscicchia, talk at THEIA-STRONG2020 Web-Seminar,20 December 2020

$K^- p$ correlation function from ALICE

P. Encarnación et al., PRD 111 (2025) 11

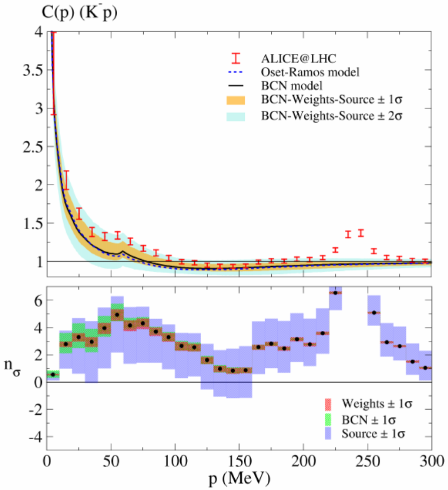

Multinucleon processes

- K^- multi-nucleon absorption in the surface region of atomic nuclei represents about 20%

  NC 53 (1968) 313 (Berkeley), *NPB 35 (1971) 332 (BNL)*, *NC 39A (1977) 538 (CERN)*

- K^- multi-nucleon absorption in atoms described by phenomenological optical potential

  E. Friedman, A. Gal, NPA 959 (2017) 66

- Model for K^-NN absorption in nuclear matter using free-space chiral amplitudes

  T. Sekihara et al., PRC 86 (2012) 065205

- New experimental data on K^-NN absorption (AMADEUS@DAΦNE)

  K. Piscicchia et al., PLB 782 (2018) 339

  R. Del Grande et al., EPJ C79 (2019) 190

- Solid microscopic model for K^-NN absorption needed!

Microscopic model for $K^- NN$ absorption in nuclear matter

Microscopic model for K^- two-nucleon absorption in symmetric nuclear matter *J. Hrtánková, À. Ramos, PRC 101 (2020) 035204*

- based on a meson-exchange approach
  H. Nagahiro et al., PLB 709 (2012) 87
- P and BCN chiral $K^- N$ amplitudes employed
- Pauli correlations in the medium for $K^- N$ amplitudes considered
- real part of the $K^- NN$ optical potential evaluated as well
- $K^- N$ optical potential derived within the same approach

$K^- N$ absorption in nuclear matter

$$K^- N \to \pi Y \quad (Y = \Lambda, \Sigma)$$

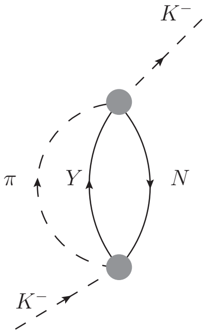

Fig.1: Feynman diagram for K^- absorption on a single nucleon in nuclear matter. The shaded circles denote the $K^- N$ t-matrices derived from a chiral model.

K^-NN absorption in nuclear matter

$$K^- + N + N \rightarrow Y + N \quad (Y = \Lambda, \Sigma)$$

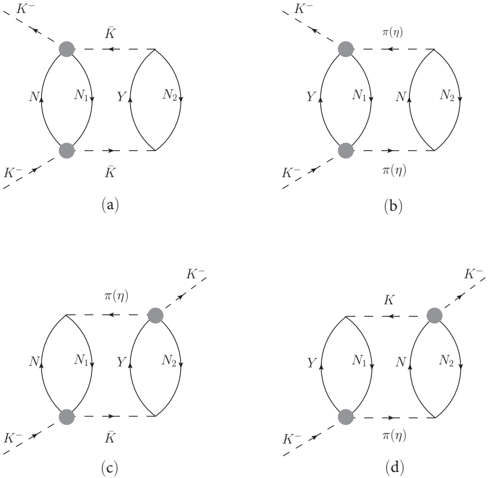

Fig.2: Two-fermion-loop (2FL) Feynman diagrams for non-mesonic K^- absorption on two nucleons N_1, N_2 in nuclear matter. The shaded circles denote the K^-N t-matrices derived from a chiral model.

K^-NN absorption in nuclear matter

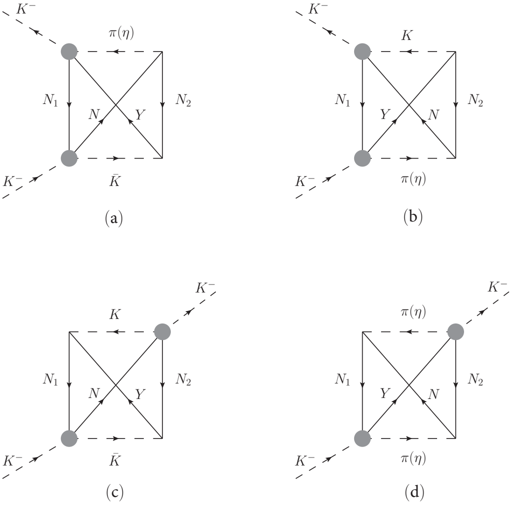

Fig.3: One-fermion-loop (1FL) Feynman diagrams for non-mesonic K^- absorption on two nucleons N_1, N_2 in nuclear matter. The shaded circles denote the K^-N t-matrices derived from a chiral model.

$K^- NN$ absorption in nuclear matter

$V_{K^-N} = \sum_{channels} V_{K^-N \to \pi Y}$ (Fig.1)

$V_{K^-NN} = \sum_{\text{channels}} V^{\text{2FL}}_{K^-NN} + V^{\text{1FL}}_{K^-NN}$ (Fig.2 and 3)

$\to$ contributions from 37 2FL and 28+33 1FL diagrams

Table 1: All considered channels for mesonic and non-mesonic K^- absorption in matter.

$K^- N$	$\to \pi Y$	$K^- N_1 N_2$	$\to YN$
$K^- p$	$\to \pi^0 \Lambda$	$K^- pp$	$\to \Lambda p$
	$\to \pi^0 \Sigma^0$		$\to \Sigma^0 p$
	$\to \pi^+ \Sigma^-$		$\to \Sigma^+ n$
	$\to \pi^- \Sigma^+$	$K^- pn(np)$	$\to \Lambda n$
$K^- n$	$\to \pi^- \Lambda$		$\to \Sigma^0 n$
	$\to \pi^- \Sigma^0$		$\to \Sigma^- p$
	$\to \pi^0 \Sigma^-$	$K^- nn$	$\to \Sigma^- n$

AMADEUS: Ratio for 2N absorption

R. Del Grande et al., EPJ C79 (2019) 190

$$R = \frac{\mathrm{BR}(K^- pp \to \Lambda p)}{\mathrm{BR}(K^- pp \to \Sigma^0 p)} = 0.7 \pm 0.2(\mathrm{stat.})^{+0.2}_{-0.3}(\mathrm{syst.})$$

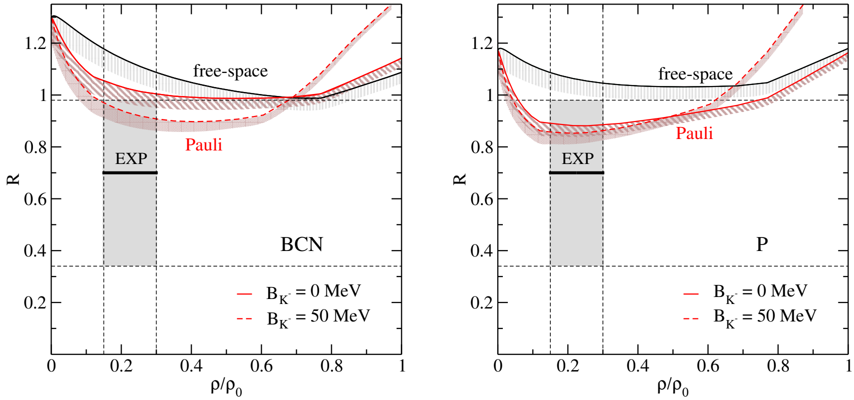

Fig.4: The ratio R as a function of relative density, calculated using the free-space and Pauli blocked amplitudes for $B_{K^-} = 0$ MeV and $B_{K^-} = 50$ MeV. Color bands denote the uncertainty due to different cut-off values $\Lambda_c =$ 800 – 1200 MeV.

Application of $K^- NN$ model to kaonic atoms

J. Óbertová, E. Friedman, J. Mareš, PRC 106 (2022) 065201

Table 2: Values of $\chi^2(65)$ resulting from comparisons of predictions with kaonic atom data using $K^- N$, $K^- N + K^- NN$, and $K^- N + K^- NN$+phen. multiN potentials. Values of complex amplitude B and parameter α for potentials based on Pauli blocked and WRW *(T. Wass, M. Rho, W. Weise, NPA 617 (1997) 449)* modified BCN amplitudes.

	$K^- N$	$K^- N + K^- NN$	+ phen.	ReB (fm)	ImB (fm)	α
Pauli	825	565	105	-1.97(13)	-0.93(11)	1.4
WRW	2378	1123	116	-0.90(9)	0.72(10)	0.6

- best fit $K^- N$ + phen. multiN potential based on BCN amplitudes ReB = -1.3 fm, ImB = 1.9 fm, $\alpha = 1$, $\chi^2(65) = 112.3$

The role of hadron self-energies

- inclusion of Y, N, K^- and π self-energies into the K^-N chiral BCN amplitudes as well as into the K^-NN model.
- considered baryon potentials

$$V_N = -\,70\frac{\rho}{\rho_0}\ \text{MeV},$$

$$V_\Lambda = -\,58\frac{\rho}{\rho_0} + 31\left(\frac{\rho}{\rho_0}\right)^2\ \text{MeV}\ \rightarrow V_\Lambda(\rho_0) = -26.4\ \text{MeV},$$

$$V_\Sigma = 30\frac{\rho}{\rho_0}\ \text{MeV}.$$

- considered pion S- and P-wave self-energy

  A. Ramos, E. Oset, NPA 671 (2000) 481

The role of hadron self-energies: $K^- p$ amplitudes

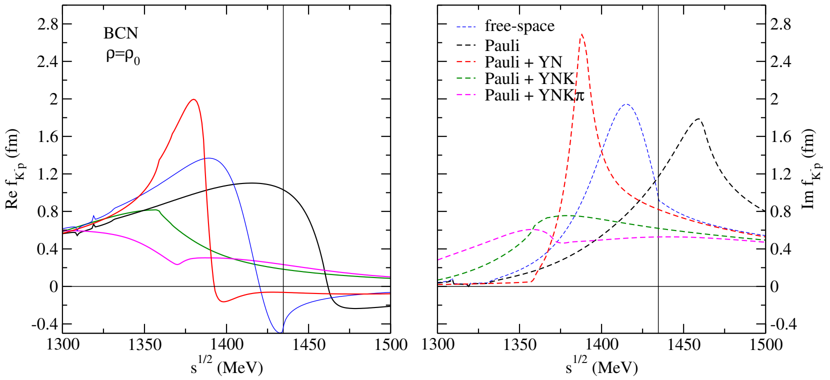

Fig.5: Comparison of $K^- p \to K^- p$ BCN amplitudes with Pauli blocking only (black), Pauli+YN SE (red), Pauli + YNK^- SE (green), and Pauli + $YNK^-\pi$ SE (magenta) at saturation density $\rho_0 = 0.17$ fm^{-3}.

The role of hadron self-energies: $K^- n$ amplitudes

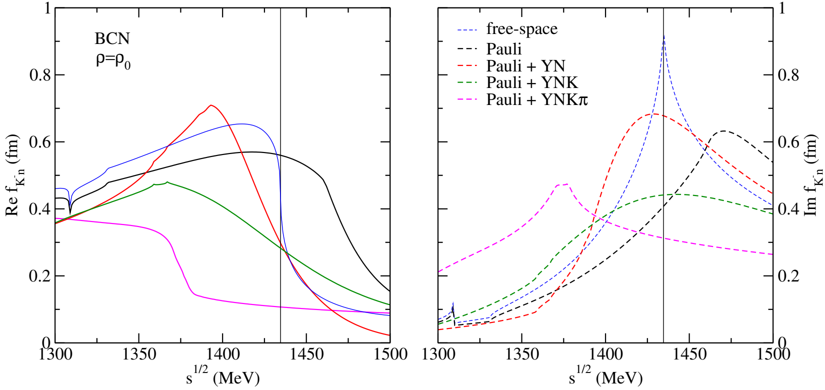

Fig.6: Comparison of $K^- n \to K^- n$ BCN amplitudes with Pauli blocking only (black), Pauli+YN SE (red), Pauli + YNK^- SE (green), and Pauli + $YNK^-\pi$ SE (magenta) at saturation density $\rho_0 = 0.17$ fm^{-3}.

Comparison with AMADEUS measurement

K. Piscicchia et al., PLB 782 (2018) 339 (AMADEUS); J.K. Kim, PRL 21 (1965) 29 (KIM)

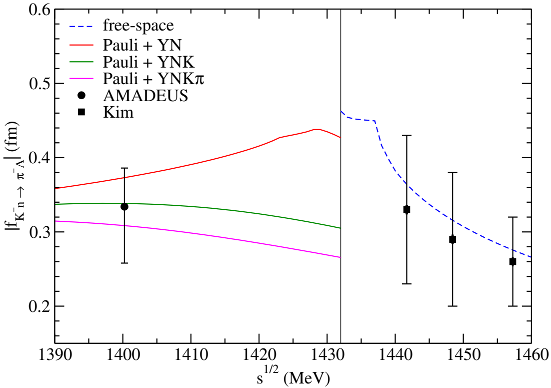

Fig.7: Comparison of $|f_{K^- n\to\pi^-\Lambda}|$ measured by AMADEUS with in-medium amplitudes: Pauli + YN SE (red), Pauli+YNK SE (green), and Pauli + $YNK^-\pi$ SE (magenta) from the BCN model (taken at $\rho = 0.3\rho_0$). For comparison there is also the corresponding free-space amplitude (blue) above threshold (vertical line) compared with the amplitude extracted from cross section data.

The role of hadron self-energies: K^- potential

- Pauli + YN SE amplitudes $\Rightarrow V_{K^-} = V_{K^-N} + V_{K^-NN}$
- Pauli + $YNK^-(YNK^-\pi)$ SE amplitudes

$$\Downarrow$$

$$V_{K^-} = t\rho + V^{\mathrm{corr}}_{K^-NN}$$

$\swarrow$ $\searrow$

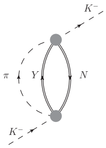

+

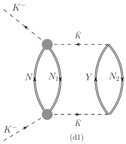

+ ... +

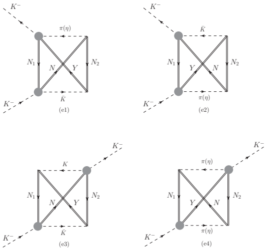

The role of hadron self-energies: K^- potential

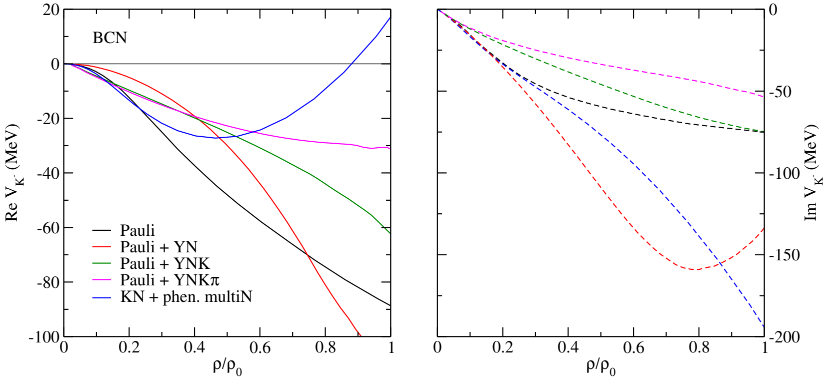

Fig.8: Real (left) and imaginary (right) parts of the total K^- potential as a function of relative density ρ/ρ_0, calculated with Pauli (black), Pauli + YN SE (red), Pauli + YNK^- SE (green), and Pauli + $YNK^-\pi$ SE (magenta) BCN amplitudes. For comparison there is the best fit K^-N + phen. multiN potential (blue) based on BCN amplitudes.

Calculations of energy shifts and widths in kaonic atoms

J. Óbertová, A. Ramos, J. Mareš, accepted in PRC (2025), arXiv:2508.07921

Table 3: Values of $\chi^2(64)$ obtained in calculations of kaonic atoms (24 nuclear species, 64 data points) using $K^- N + K^- NN$ potentials based on BCN Pauli, Pauli+YN, Pauli+YNK, and Pauli+YNKπ amplitudes. For comparison, there are also results of calculations with $K^- N$+phen. multiN potential based on WRW modified BCN amplitudes *(T. Wass, M. Rho, W. Weise, NPA 617 (1997) 449)*.

BCN	Pauli	Pauli+YN	Pauli+YNK	**Pauli+YNKπ**	WRW
	$K^- N + K^- NN$	$K^- N + K^- NN$	$t\rho + V^{corr}_{K^- NN}$	$t\rho + V^{corr}_{K^- NN}$	$K^- N$+phen. multiN
$\chi^2(64)$	553.2	265.5	169.2	**96.0**	122.0
χ^2/d.p.	8.6	4.2	2.6	**1.5**	1.9

- A. Baca et al. *(NPA 673 (2000))* obtained value of $\chi^2/dof = 3.8$ with K^- potential based on chiral model of Oset and Ramos *(NPA 671 (2000))*.

Total K^- potential in ^{12}C+K^- and ^{208}Pb+K^- atoms

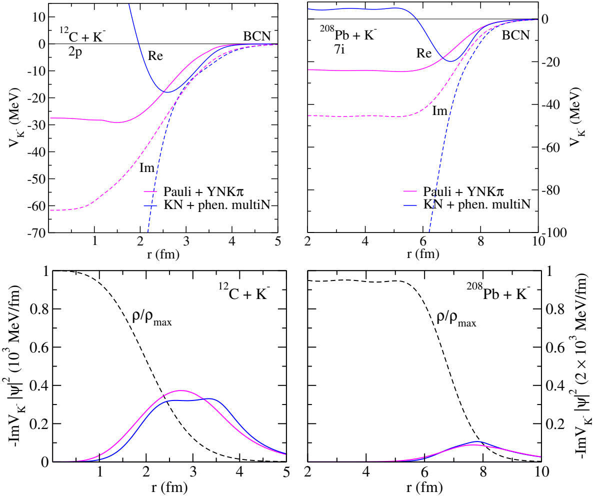

Fig.9: Total K^- potential in kaonic carbon (left) and kaonic lead (right) calculated with the Pauli+YNKπ BCN amplitudes (magenta) compared with the K^-N+phen. multiN potential (blue) based on the BCN amplitudes. Lower panel shows the corresponding overlap of ImV_{K-} with the K^- wave function squared $|\psi|^2$.

Branching ratios in ^{12}C+K^- atom

Table 4: Primary-interaction branching ratios (in %) for mesonic ($K^-N \to Y\pi$, $Y = \Lambda, \Sigma$) and non-mesonic absorption ($K^-NN \to YN$) of K^- in ^{12}C+K^- atom (3d level), calculated with total K^- potential based on Pauli + YNKπ BCN amplitudes. The experimental data corrected for primary interaction are shown for comparison.

^{12}C + K^- (3d)	BCN		Exp.			
mesonic ratio	Pauli+YNKπ	Sum	[1]	Sum	[2]	Sum
$\Sigma^+\pi^-$	14.4	33.7	29.4 $\pm$ 1.0	38.8$\pm$1.2	14.4 $\pm$ 2.3	39.2$\pm$3.0
$\Sigma^0\pi^-$	8.2		2.6 $\pm$ 0.6		1.2 $\pm$ 0.4	
$\Lambda\pi^-$	11.1		6.8 $\pm$ 0.3		23.6 $\pm$ 1.9	
$\Sigma^-\pi^0$	8.1	23.4	2.6 $\pm$ 0.6	26.0$\pm$0.9	1.2 $\pm$ 0.4	24.8$\pm$1.8
$\Sigma^0\pi^0$	10.0		20.0 $\pm$ 0.7		11.8 $\pm$ 1.4	
$\Lambda\pi^0$	5.3		3.4 $\pm$ 0.2		11.8 $\pm$ 1.0	
$\Sigma^-\pi^+$	12.8		13.1 $\pm$ 0.4		10.3 $\pm$ 1.7	
total 1N ratio (3d)	70.0		77.9 $\pm$ 1.6		74.3 $\pm$ 3.9	
total 1N ratio (3d + 4f)	71.8					
total multiN ratio (3d)	30.0		19.0 $\pm$ 2.0		25.7 $\pm$ 3.1	
total multiN ratio (3d + 4f)	28.2			27 $\pm$ 3(stat.)$^{+5}_{-6}$(syst.) [3]		

[1] *C. Vander Velde-Wilquet et al., NC 39 A (1977) 538*

[2] *H. Davis et al., NC 53 A (1968) 313*

[3] *R. Del Grande et al., PS 95 (2020) 084012*

Summary

- $K^- N$ interaction described by chiral meson-baryon coupled channel interaction models
- Interactions of K^- with two and more nucleons important for realistic description of the K^--nucleus interaction
  - only P, KM, and BCN models compatible with available data
- We have developed a microscopic model for $K^- NN$ absorption in nuclear matter using amplitudes derived from the P and BCN chiral meson-baryon interaction models

  J. Hrtánková, À. Ramos, PRC 101 (2020) 035204
  - Pauli blocked amplitudes included $\rightarrow$ medium effects non-negligible
  - Calculated ratios in a good agreement with experimental data

Summary

- Further extension of the $K^- NN$ model and $K^- N$ BCN amplitude model $\rightarrow$ inclusion of hadron (Y, N, K^-, π) self-energies
- Considering all hadron SE $\rightarrow \mathrm{Re}\, V_{K^-}(\rho_0) \sim -30$ MeV and $\mathrm{Im}\, V_{K^-}(\rho_0) \sim -50$ MeV
- Calculations of energy shifts and widths in kaonic atoms:
  - inclusion of $K^- NN$ absorption improves the description of data considerably

    J. Óbertová, E. Friedman, J. Mareš, PRC 106 (2022) 065201
  - **full model Pauli+$YNK\pi$ SE describes the data as good as the best fit $K^- N$+phen. multiN potential based on BCN amplitudes!**

    J. Óbertová, A. Ramos, J. Mareš, accepted in PRC (2025), arXiv:2508.07921

BACK-UP SLIDES

Total K^- potential: version 2025 vs. 2000

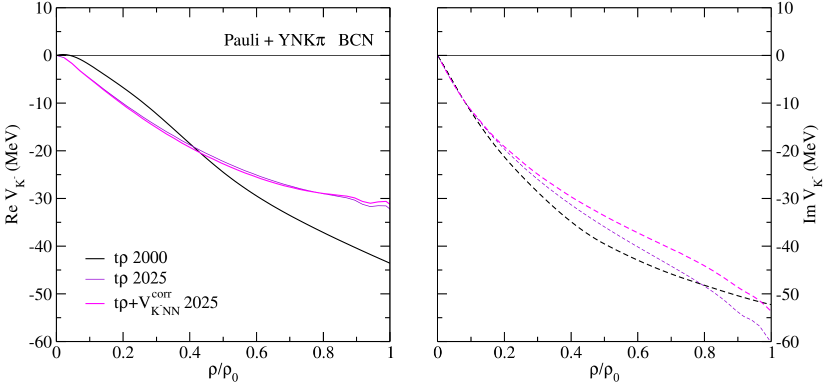

Fig.10: Real (left) and imaginary (right) parts of the total K^- potential calculated with Pauli + YNKπ (magenta) BCN amplitudes compared with the K^- optical potential including hadron SE based on the model of Oset and Ramos (black). Thin violet lines represent the $t\rho$ part of the current K^- optical potential obtained with Pauli YNKπ BCN amplitudes.

Branching ratios from FINUDA

Table 5: Primary-interaction ratios (in %) for the $\Sigma^-\pi^+$ and $\Sigma^+\pi^-$ channels in light kaonic atoms calculated using the Pauli+YNKπ BCN amplitudes. Experimental data from the FINUDA collaboration [4] are corrected for pion attenuation and for $\Sigma N - \Lambda N$ conversion with probabilities (a) 60 % for Σ^+ and 22.5 % for Σ^- (b) 50 % for both Σ's.

	BCN		Exp. [4]			
	Pauli+YNKπ		(a)		(b)	
nucleus (nl)	$\Sigma^+\pi^-$	$\Sigma^-\pi^+$	$\Sigma^+\pi^-$	$\Sigma^-\pi^+$	$\Sigma^+\pi^-$	$\Sigma^-\pi^+$
^{6}Li ($2p+3d$)	16.1	17.5	45.8 $\pm$ 4.3	19.4 $\pm$ 1.5	36.7 $\pm$ 3.4	30.0 $\pm$ 2.3
^{7}Li ($2p+3d$)	12.6	11.0	20.5 $\pm$ 1.4	8.7 $\pm$ 1.0	16.4 $\pm$ 1.1	13.4 $\pm$ 1.5
^{9}Be ($3d$)	13.1	12.6	14.6 $\pm$ 1.1	5.9 $\pm$ 0.7	11.7 $\pm$ 0.9	9.2 $\pm$ 1.2
^{12}C^a ($3d$)	14.7	13.2	25.0 $\pm$ 0.8	10.2 $\pm$ 0.3	20.0 $\pm$ 0.7	15.9 $\pm$ 0.4
^{13}C ($3d$)	12.7	10.3	18.6 $\pm$ 2.7	6.5 $\pm$ 0.8	14.9 $\pm$ 2.2	10.1 $\pm$ 1.2
^{16}O ($3d$)	14.5	11.6	19.3 $\pm$ 1.9	8.4 $\pm$ 0.8	15.5 $\pm$ 1.5	13.0 $\pm$ 1.2

[a] Branching ratios for ^{12}C were measured in bubble chamber experiment [1] but they served as reference values in Table 1 in Ref. [4].

[4] *M. Agnello et al., PLB 704 (2011) 474*

K^- absorption probabilities in p-shell nuclei

S. Manti, cascade calculations